

NACA RM E51E04

E 51 E 04

TECH LIBRARY KAFB, NM
0143200

NACA

RESEARCH MEMORANDUM

INVESTIGATION OF INTERNAL FILM COOLING OF 1000-POUND-THRUST
LIQUID-AMMONIA - LIQUID-OXYGEN ROCKET-ENGINE
COMBUSTION CHAMBER

By Gerald Morrell

Lewis Flight Propulsion Laboratory
Cleveland, Ohio

John B.

NATIONAL ADVISORY COMMITTEE
FOR AERONAUTICS

WASHINGTON
July 17, 1951

319.98/13



0143200

NACA RM E51E04

~~CONFIDENTIAL~~

NATIONAL ADVISORY COMMITTEE FOR AERONAUTICS

RESEARCH MEMORANDUMINVESTIGATION OF INTERNAL FILM COOLING OF 1000-POUND-THRUST
LIQUID-AMMONIA - LIQUID-OXYGEN ROCKET-ENGINE COMBUSTION CHAMBER

By Gerald Morrell

SUMMARY

Internal film cooling of the combustion chamber of a 1000-pound-thrust liquid-ammonia - liquid-oxygen rocket engine was investigated. Chamber pressure varied between 220 and 270 pounds per square inch absolute. The three coolants studied were water, 2 to 7.5 percent of total flow; ethyl alcohol, 5 to 15 percent of total flow; and liquid ammonia, 3 to 21 percent of total flow.

Gas-to-coolant film heat-transfer data are presented and compared with data previously obtained in a water-cooled, 4-inch-diameter steady-flow film-cooling duct. For comparable gas-stream conditions and coolant flows, the film-cooled surface in the rocket engine was found to be as much as twice that predicted from the burner data. In order to cool the 8.5-inch-long, 4-inch-diameter test section of the combustion chamber completely, a flow of water equal to approximately 5 percent of total flow through the engine was required; when ethyl alcohol was used, a flow of approximately 15 percent of total flow was required; and when ammonia was used, a flow of approximately 9 percent of total flow was required.

Performance of the ammonia-oxygen system was determined in an uncooled engine having the same dimensions as the cooled engine. The data, which were corrected to a chamber pressure of 250 pounds per square inch absolute, indicate a maximum specific impulse of 220 pound-seconds per pound at an oxidant-fuel ratio of 1.4 (stoichiometric ratio = 1.41). Over a range of oxidant-fuel ratios from 1.1 to 1.6, the effect of film cooling on performance is a 4 percent reduction in specific impulse for a water-coolant flow of 5 percent of total flow, a 4 percent reduction in specific impulse for an alcohol-coolant flow of 15 percent, no reduction in specific impulse for an ammonia-coolant flow up to 11 percent, and only a 2 percent reduction in specific impulse for an ammonia-coolant flow of 15 percent.

~~CONFIDENTIAL~~
MANENT
RECORD

INTRODUCTION

The extremely high temperatures and rates of heat transfer encountered in rocket engines pose a very difficult cooling problem. Regenerative or external cooling is one approach to the solution of this problem. Another and perhaps more promising approach is internal cooling, which involves the maintenance of a buffer layer of coolant between the hot gas and the engine wall. Lower inner-wall temperatures, lower overall pressure drops, and lower power-plant weights are to be expected when internal rather than regenerative cooling is used. For some of the high-energy propellants now being considered, the properties of which make them unsuitable for regenerative cooling, it appears that internal cooling may be the only adequate method; reference 1 indicates that internal cooling can prevent build up of oxides on the engine wall when metallic fuels are used.

If the walls of an engine are constructed of a porous material, the coolant fluid can be forced through the wall to form a protective boundary layer on the inner surface; this is known as transpiration or sweat cooling (references 2 to 6). A disadvantage of this method is the difficulty of obtaining uniform flow through large sections. If liquid coolants are used (reference 7), vapor lock may limit the flow through the wall.

Film cooling involves the introduction of a coolant at discrete points along the inner wall of the combustion chamber and allowing the hot gases to sweep the coolant downstream to form a protective layer. This method is especially promising with liquids if the latent heat of vaporization can effectively be utilized; at least one manufacturer is developing an engine using this method of cooling in the combustion chamber. Film cooling with water considerably reduces nozzle-wall temperatures in an acid-aniline rocket engine (reference 8). Film cooling with water in a hydrogen-oxygen flame tube is reported in reference 9, but because an excess of water was used no heat-transfer data were obtained. A study of film cooling with water in an acid-aniline rocket engine that was also regeneratively cooled and showed a marked decrease in heat transfer to the external coolant is reported in reference 10. Gas-to-liquid film heat-transfer rates were established by studying steady-state cooling in a 4-inch-diameter duct film cooled with water at air temperatures to 2000° F (reference 11). The Stanton number was found to be proportional to a function of Reynolds number and Prandtl number for a given coolant flow.

The present investigation of a 1000-pound-thrust liquid-ammonia - liquid-oxygen rocket engine was undertaken to determine if the preliminary correlation previously obtained in the steady-state burner

(reference 11) would apply to a rocket engine, to establish the effectiveness of fuels as film coolants in the absence of simultaneous regenerative cooling, and to measure the effect of film cooling on performance. A noncarbonaceous propellant system was chosen to simplify radiation calculations and to prevent carbon formation on the test-section walls. The coolant, either water, ethyl alcohol, or anhydrous liquid ammonia, was circumferentially introduced at the upstream end of a thin-walled section of the chamber; skin thermocouples indicated the effectively cooled length. The work reported herein was conducted at the NACA Lewis laboratory during 1950.

SYMBOLS

The following symbols are used in this report:

- $c_{p,g}$ specific heat at constant pressure of combustion gas in test section, (Btu/(lb)(°F))
- $c_{p,l}$ average specific heat at constant pressure of liquid coolant, (Btu/(lb)(°F))
- D diameter of film-cooled test section, (ft)
- F engine thrust, (lb force)
- G mass velocity of combustion gas, (lb/(sec)(sq ft))
- H heat of vaporization of coolant, (Btu/lb)
- h heat-transfer coefficient, (Btu/(sec)(sq ft)(°F))
- I specific impulse of rocket engine, $\frac{\text{thrust, (lb force)}}{\text{total flow rate, (lb/sec)}}$
- k thermal conductivity, (Btu/(sec)(sq ft)(°F/ft))
- L liquid film-cooled length, (ft)
- M molecular weight
- N_{Pr} Prandtl number, $\frac{c_p \mu}{k}$
- N_{Re} Reynolds number, $\frac{DG}{\mu}$
- n_i weight fraction of i^{th} component

P_c	chamber pressure, (lb/sq in. abs.)
P_o	ambient pressure, (lb/sq in. abs.)
q_c	convective heat transfer per pound of coolant, (Btu/lb)
q_r	radiation heat transfer per pound of coolant, (Btu/lb)
q_t	total heat transfer per pound of coolant, (Btu/lb)
R_I	impulse ratio with cooling, $\frac{\text{experimental specific impulse (cooled)}}{\text{experimental specific impulse (uncooled)}}$
T_f	theoretical flame temperature, ($^{\circ}\text{R}$)
T_g	total temperature of combustion gas, ($^{\circ}\text{R}$)
T_s	temperature of surface of liquid coolant, ($^{\circ}\text{R}$)
T_w	inside-wall temperature, ($^{\circ}\text{R}$)
W_f	fuel flow, (lb/sec)
W_g	average flow of combustion gas through test section, $W_o + W_f + \frac{W_l}{2}, \quad (\text{lb/sec})$
W_l	liquid-coolant flow, (lb/sec)
W_o	oxidant flow, (lb/sec)
γ	ratio of specific heats
η_I	impulse efficiency, $\frac{\text{experimental specific impulse}}{\text{theoretical specific impulse}}$
μ	viscosity, (lb/(sec)(ft))
ρ	density of gas, (lb/cu ft)

APPARATUS AND PROCEDURE

Apparatus

A diagrammatic sketch of the rocket engine used in this investigation is presented in figure 1. The engine consists of the following components: propellant injector, adapter section, coolant injector, thin-walled test section, and solid copper nozzle, which was chrome plated on the hot-gas side. The propellants and the coolant were introduced into the engine through electrically actuated gas-operated valves from pressurized storage tanks.

Propellant injector. - The propellant injector used in this investigation, produced 24 fuel jets that impinged on 12 oxidant jets at a distance of approximately 0.75 inch from the injector face, the fuel being on the outside (fig. 2). In an attempt to improve combustion efficiency and operational simplicity, two injectors, each having 24 pairs of jets impinging about 0.375 inch from the injector face with oxidant on the outside, were tried. One of these injectors was equipped for gunpowder-squib ignition and the other for spark-plug ignition. Use of these injectors resulted in screaming operation that destroyed the coolant film and caused the test section to become overheated. Performance tests showed that these injectors did not produce improved impulse efficiency over that obtained with the standard injector.

A 4-inch inside-diameter heavy-walled adapter, 2.8-inches long, between the propellant injector and the coolant injector was used as a means of mounting the engine on the thrust stand.

Coolant injectors. - Three types of coolant injector were used in this investigation. The first injector was the same as the jet-type injector described in reference 11. Frequent clogging of the No. 80 drill holes caused nonuniform cooling even with two filters in the coolant line. The second injector (vertical-slot injector) had a divided stainless-steel insert, one-half of which had an integral deflector ring, 1/2-inch long. The other half had 60 rectangular slots, 0.005-inch deep and 0.062-inch wide, directed perpendicularly to the deflector ring, as shown in figure 3. The third injector had the slots cut at 45° angles to the axis and directed tangentially at the deflector ring. Because this tangential-slot injector failed to improve cooling effectiveness, it was used for only a few of the runs.

Test section. - The stainless-steel test section, shown in figure 4, consisted of a 4-inch inside-diameter tube, approximately 8.5-inches long, with a wall thickness of 0.095 inch. The 34 chromel-alumel skin thermocouples were attached in several rows in order to

obtain circumferential as well as longitudinal temperature distributions. The exact arrangement of these thermocouples was as follows:

Distance downstream of test-section entrance (in.)	Number of thermocouples	Circumferential spacing of thermocouples (deg)
1	2	180
2	2	180
3	2	180
4	4	90
5	4	90
6	4	90
7	8	45
7.5	8	45
Total 34		

Exhaust nozzle. - A convergent-divergent nozzle, machined from a solid copper billet and chrome plated on the hot-gas side, completed the rocket engine assembly. This nozzle, designed for an expansion ratio of 20.4, had the following dimensions: throat diameter, 1.875 inches; exit diameter, 3.86 inches; throat- to exit-area ratio, 0.236; convergence half angle, 30° ; divergence half angle, 15° .

Ignition system. - Ignition was accomplished by means of a coaxial cable arranged to form a spark gap at the open end. This cable, powered by a high-voltage transformer, was inserted through the nozzle into the chamber and held in place by a metal spring. After ignition, the expanding gas ejected cable and spring from the engine.

Propellants and coolants. - Commercial liquid oxygen and anhydrous liquid ammonia were used as propellants; the ammonia was used as a coolant as well. Water for film cooling was taken from city mains and filtered twice before reaching the coolant injector. The specially denatured alcohol used as a coolant assayed 95-percent ethyl alcohol and 5-percent methyl alcohol.

Instrumentation. - Propellant flow was continuously measured with an accuracy of ± 1 percent by strain gages attached to counter-balanced weighing beams; the output of the gages was fed to self-balancing recording potentiometers. Coolant flow was measured with an accuracy of ± 0.02 pound per second by an area-type transmitter and recorder; the recorder was placed as near as practicable to the transmitter to keep transmission lines to a minimum.

Engine thrust was measured with an accuracy of ± 10 pounds by a strain gage unit attached to the parallelogram thrust stand; the output of the gage was fed to a self-balancing recording potentiometer.

Chamber pressure was measured with an accuracy of ± 6 pounds per square inch by a Bourdon-tube type strip-chart recorder located near the engine to keep hydraulic lines to a minimum.

The outputs of 12 chromel-alumel thermocouples on the test-section surface were measured and recorded by self-balancing potentiometers with an accuracy of ± 0.125 millivolt in the 10-millivolt range and an accuracy of ± 0.2 millivolt in the 20-millivolt range. Outputs of eight additional chromel-alumel thermocouples on the test-section surface were recorded by a single-channel oscillograph with an accuracy of ± 0.2 millivolt by means of a high-speed automatic-selector switch making 10 contacts per second.

Procedure

After the propellant and coolant tanks were loaded, the igniter cable was inserted into the engine. The coolant line was bled at the control valve so that coolant would enter the engine ahead of the main propellants and then the tanks were pressurized. The firing procedure consisted in turning on the instruments and then the igniter. Propellant and coolant control valves were then simultaneously opened.

Running time varied between 5 and 30 seconds depending on whether the coolant flow was chosen to partially or completely cool the chamber test section. Because a single run without coolant caused a chamber burnout in less than 5 seconds, 30 seconds was considered a long enough period of time to establish that the test section was stably and completely cooled.

For determination of performance without cooling, a heavy-walled chamber was substituted for the adapter, coolant injector, and test section. The characteristic length of the resultant configuration was approximately 67 inches, compared with 64 inches for the film-cooled engine.

Liquid-cooled length. - The liquid-cooled length is the distance downstream of the coolant injector that the film of liquid coolant persists on the chamber wall. This distance was determined by plotting outside-wall temperature against distance from the test-section entrance. If different rows of thermocouples disagreed, the average of the several curves was taken. Calculations, in which equations recommended by McAdams in reference 12 were used, showed that the heat loss

by free convection and radiation from the test-section surface to the ambient air was so small at an outside-wall temperature of 300° F that the measured outside-wall temperature could be used without appreciable error in place of the inside-wall temperature throughout the cooled portion of the chamber.

The slope of the temperature-distance curve increased sharply beyond the point where the wall temperature equals the boiling temperature of the coolant at the measured chamber pressure for both water and alcohol cooling. The distance from the test-section entrance to the point at which the outside-wall temperature equals the boiling temperature of the coolant was taken as the liquid-cooled length.

When liquid ammonia was used as a coolant, the temperature-distance curves were quite different from the water and alcohol curves just discussed. In this case, there was no sharp change in slope when the wall temperature reached the boiling temperature of the coolant; instead the temperature along the test section gradually increased. In order to determine the liquid-cooled length, it was assumed that the ammonia on the wall existed as a superheated liquid up to the point at which the wall temperature was equal to 270° F, the critical temperature of ammonia. The small additional cooling obtained beyond this point, presumably by gaseous ammonia, was disregarded except in the determination of the minimum quantity of ammonia required to cool the entire test section.

Reduction of cooling data. - Heat-transfer data were obtained by using coolant flows that were less than the minimum required to cool the entire test section. These runs were necessarily of short duration, 10 seconds or less, but the pressure, thrust, and temperature records indicated that steady-state operation was attained. The Reynolds number of the combustion gas could not be varied appreciably; therefore, an independent heat-transfer correlation was not possible. It was assumed that the correlation reported in reference 11 for a gasoline-air burner film-cooled with water would be valid in this case. The equation for this correlation may be written

$$\frac{h}{c_{p,g} G} = a \left(\frac{DG}{\mu_g} \right)^{0.07} \left(\frac{c_{p,g} \mu_g}{k_g} \right)^{-0.6} \quad (1)$$

where the proportionality constant varies with coolant flow.

For the experimental conditions involved, h is defined as

$$h = \frac{q_c W_L}{(\pi D L)(T_g - T_s)} \quad (2)$$

Substituting equation (2) in equation (1) and rearranging yields

$$W_L = a W_g \left[\frac{c_{p,g}(T_g - T_s)}{q_c} \right] \left(\frac{4L}{D} \right) N_{Re}^{0.07} N_{Pr}^{-0.6} \quad (3)$$

This equation was used to generalize all heat-transfer data obtained.

The physical properties of the combustion gases were calculated from the theoretical compositions by means of the following equations recommended in reference 13:

$$c_{p,g} = \sum n_i c_{p,i} \quad (4)$$

$$k_g^{0.4} = \sum n_i k_g^{0.4} \quad (5)$$

$$\left(\frac{\rho}{\mu} \right)_g = \sum n_i \left(\frac{\rho}{\mu} \right)_i \quad (6)$$

Theoretical compositions were calculated by the method of reference 14 with the assumption that the propellants were liquid; the results were found to agree substantially with the compositions listed in reference 15 where one of the propellants is assumed to be gaseous. For molecular species, values of μ were taken from reference 16 and logarithmically extrapolated. Values of k were computed by means of the Eucken equation (reference 17): $k = \frac{(9\gamma - 5)(\mu)(c_p)}{4\gamma}$. For free radicals, values of k and μ were taken from reference 18. For all species, values of c_p were taken from reference 19 and values of ρ were calculated from the ideal-gas equation. In figure 5, the physical properties of the combustion gas, calculated on the basis of theoretical composition, are plotted as functions of oxidant-fuel ratio.

The total gas temperature was calculated from the impulse efficiency on the assumption that γ and M did not appreciably differ from the theoretical values and that P_0 was 1 atmosphere for the actual case. From the relation obtained by using equations of reference 20,

$$I \propto \left\{ \left(\frac{T_f}{M} \right) \left[1 - \left(\frac{P_0}{P_c} \right)^{\frac{r-1}{r}} \right] \right\}^{\frac{1}{2}}$$

the following equation can be derived:

$$T_g = \eta_I^2 T_f \quad (7)$$

Theoretical values of specific impulse, flame temperature, and ratio of specific heats are shown in figure 6. Flame temperature and ratio of specific heats were calculated by the method of reference 14. Specific impulse was calculated in the same way by assuming equilibrium, isentropic, one-dimensional flow through the expansion nozzle.

The convective heat transfer per pound of coolant was calculated from

$$q_c = q_t - q_r \quad (8)$$

where

$$q_t = c_{p,l} (T_s - T_w) + H \quad (9)$$

This expression neglects the heat transfer from the liquid film to the retaining wall and the heat conduction from the hotter to the cooler sections of the retaining wall. Calculations indicated that these quantities were of the order of 1 Btu per pound of coolant as compared with a total heat transfer of several hundred Btu per pound of coolant. Values of q_c , q_r , and q_t are given in tables I and II.

For water and ethyl alcohol, T_s was taken as the boiling temperature of the liquid at the indicated chamber pressure and for T_w the measured outside-wall temperature was used. For ammonia, T_s was arbitrarily taken as the average outside-wall temperature because T_s could not be assigned with any degree of certainty from the data obtained; T_w was taken as 80° F, which was assumed to be the temperature of issuance from the injector.

Specific-radiation heat transfer was calculated by the method presented in reference 21. No effect of pressure on gas emissivity and an emissivity of 0.9 for the coolant surface were assumed. For runs in

~~CONFIDENTIAL~~

2178

which alcohol was used as a coolant, the effect of the products of combustion of alcohol on the gas emissivity was taken into account.

Reduction of performance data. - All performance data, with or without cooling, were reduced for comparison purposes to a common value of chamber pressure of 250 pounds per square inch absolute by assuming that T_F/M did not vary with moderate changes in chamber pressure. Then,

$$I \propto \left[1 - \left(\frac{P_0}{P_c} \right)^{\frac{\gamma-1}{\gamma}} \right]^{\frac{1}{2}}$$

where γ is obtained from figure 6.

RESULTS AND DISCUSSION

Heat-Transfer Results

The pertinent heat-transfer data and the associated performance data obtained are tabulated in tables I and II. In table I, the theoretical specific impulse is based on an oxidant-fuel ratio which does not include the coolant water. It was assumed that the water acts as an inert substance in the combustion process. For the case in which fuel was used as a coolant (table II), the theoretical specific impulse was based on an oxidant-fuel ratio which included the fuel coolant. In all cases, the experimental specific impulse was based on total flow through the engine.

The oxidant-fuel ratio was varied between 0.8 and 2.0, the chamber pressure varied between 220 and 270 pounds per square inch absolute, and the coolant flows were within the following ranges: water, 2 to 7.5 percent of total flow; ethyl alcohol, 5 to 15 percent; and ammonia, 3 to 21 percent.

Liquid Film-Cooled Length

Temperature-distance curves. - Typical outside-wall temperature - distance curves are shown in figures 7 and 8 for water, alcohol, and ammonia cooling. The symbols refer to various longitudinal rows of thermocouples around the circumference of the test section. For water

and alcohol, the sharp change in slope corresponding to expiration of the film can readily be seen in figures 7(a) and 7(b). In figure 8(b) for ammonia cooling, no such break occurs, but rather a gradual increase in temperature with distance downstream of the test-section entrance. This indicates the necessity of arbitrarily using the critical temperature of ammonia as the maximum temperature of the liquid film. Another reason for selecting an arbitrary temperature limit for the liquid-ammonia coolant film is that stable temperatures higher than the boiling point of ammonia at the measured chamber pressure are attained over considerable portions of the test section. A possible explanation for this phenomenon is that the combustion gases near the cool-liquid boundary are fuel rich; this would decrease the ammonia-concentration gradient between the liquid surface and the main gas stream thereby hindering diffusion of ammonia vapor away from the liquid surface. This decrease in rate of diffusion would favor the tendency of the liquid to become superheated, which would account for wall temperatures being higher than the equilibrium boiling temperature.

Where different rows of thermocouples indicated different cooled lengths, the indicated lengths of the rows were averaged (fig. 7(a)) or an average line was drawn through the points (fig. 8(b)).

Coolant flow required to cool entire length of test section. - A quantity of water equal to approximately 5 percent of total flow was just sufficient to cool the entire length of the test section ($L/D = 2.125$); with ammonia, this value was approximately 9 percent; and with ethyl alcohol, about 15 percent of total flow was required.

The ammonia flow of 9 percent is based on an outside-wall temperature of 350°F , which was the highest steady-state temperature attained in runs during which the test section was cooled throughout its entire length.

Film-cooled length as a function of coolant flow. - The relations between the liquid-cooled length to diameter ratio and the percentage coolant flow are shown in figure 9 for the three coolants studied. As in reference 11, the cooling effectiveness of ammonia (fig. 9(c)) is greater at lower coolant flows; alcohol (fig. 9(b)) shows a somewhat similar trend. This improved cooling effectiveness indicates the desirability of using a multiplicity of coolant injectors, rather than relying on one injector to cool the entire chamber.

In the flow range investigated, water does not follow this trend. It is possible, however, that extension of the data to higher flows would result in a decrease in efficiency as with the fuels, but to prove this would require a much longer test section (reference 11) than was used in this investigation.

Correlation of Heat-Transfer Data

All the heat-transfer data obtained are plotted in figure 10 in accordance with equation (3). The slope of the curves decreases as coolant flow increases; thus, a given increment of coolant flow in the high-flow region will produce a smaller percentage change in film-cooled length than the same increment in the low-flow region, if other variables are held constant. For the same gas-stream conditions, the actual cooled area in the rocket engine is as much as double the area which would be predicted from the burner data of reference 11 over the applicable coolant-flow range. It is probable that a more accurate estimation of total specific heat transfer for the ammonia coolant would reduce the difference of the rocket-engine data. Because the ammonia may be superheated, a small temperature gradient through the liquid film would be expected. Hence, the value of $T_g - T_w$ would probably be less than $T_w - 80$, which was used in equation (9). Furthermore, T_g being greater than T_w , the true heat of vaporization would be lower than the value used. The true total heat transfer per pound of coolant q_t and hence the convective component q_c would in turn be lower, which would give rise to higher ordinate values for ammonia in figure 10, and bring them into closer agreement with the values for water and alcohol.

Although it is of limited scope, figure 10 may be used to approximate film-cooling requirements for a cylindrical rocket-engine chamber when the propellant injector design approximates that used in this investigation. An example of the use of figure 10 for design purposes should serve to clarify the significance of the curves presented.

Assume a 1000-pound thrust ammonia-oxygen rocket engine with a cylindrical chamber 4 inches in diameter to be film cooled with ammonia. Further, assume an aspect ratio of the chamber of 1 ($L/D = 1$), an oxidant-fuel ratio of 1.3, and a chamber pressure P_c of 300 pounds per square inch absolute. The problem is to determine the amount of ammonia required to completely cool the chamber if the peripheral coolant injector is an integral part of the propellant injector. An experimental specific impulse of 231 pound seconds per pound at a chamber pressure of 300 pounds per square inch absolute in a 200-pound-thrust engine is reported in reference 22. The corresponding theoretical specific impulse is 257 pound seconds per pound and the theoretical flame temperature is 4880° F.

According to equation (7),

$$T_g = 3850^\circ \text{ F}$$

From figure 5,

$$c_{p,g} = 0.98 \text{ Btu}/(\text{lb})(^{\circ}\text{F})$$

$$k_g = 45.4 \times 10^{-6} \text{ Btu}/(\text{ft})(\text{sec})(^{\circ}\text{F})$$

$$\mu_g = 53 \times 10^{-6} (\text{lb})/(\text{ft})(\text{sec})$$

$$N_{Pr} = 1.15$$

Assume that $T_i = 150^{\circ}\text{F}$ and that the coolant temperature at the injector is 80°F , then $q_t = 500 \text{ Btu per pound (reference 16)}$.

On the basis of the results of this investigation, take $q_r = 0.1 q_t$, so that $q_c = 450 \text{ Btu per pound of coolant}$. As a first approximation, take W_g as equal to $W_o + W_f = 1000/231 = 4.33 \text{ pounds per second}$. Then,

$$W_g \left[\frac{c_{p,g}(T_g - T_s)}{q_c} \right] \left(\frac{4L}{D} \right) N_{Re}^{0.07} N_{Pr}^{-0.6}$$

$$= 4.33 \left[\frac{0.98(3700)}{450} \right] (4) (3.12 \times 10^5)^{0.07} (1.15)^{-0.6} = 312$$

From figure 10, $W_l = 0.24 \text{ pounds per second}$ or 12.8 percent of the total flow of fuel is the approximate amount to be used as a coolant along the wall to absorb the heat transferred by forced convection. If a better estimate is desired, adjust W_g , calculate q_r by Hottel's method (reference 21), and perform the calculation a second time.

Effect of Film Cooling on Performance

Performance data for the ammonia-oxygen system, obtained in an uncooled engine and corrected to 250 pounds per square inch absolute chamber pressure, are plotted in figure 11 and indicate a maximum specific impulse of 220 pound seconds per pound at an oxidant-fuel ratio of 1.4 (stoichiometric ratio = 1.41). The engine used to obtain these data had a characteristic length of 67 inches and was equipped with the same propellant injector and nozzle that were used for the cooling experiments.

The performance of the film-cooled engine, reduced to 250 pounds per square inch absolute chamber pressure, is compared with the performance of the uncooled engine on the basis of the impulse ratio with cooling R_I , and coolant flow $100 W_L/(W_O+W_F+W_L)$ in figure 12.

Despite considerable scatter in the data, it is possible to draw several conclusions about the effect of film cooling on performance.

With water as a coolant (fig. 12(a)), the data indicate a decrease in impulse ratio with increasing coolant flow in the range of mixture ratios from 1.1 to 1.6; for example, at a 5-percent coolant flow, specific impulse is reduced approximately 4 percent. For mixture ratios greater than 1.6, no decrease in impulse ratio was obtained with increasing coolant flow. This phenomenon, together with the occasional appearance of ratios greater than unity, may be due in large part to experimental error and in part to the fact that the addition of water in the oxygen-rich regime would tend to reduce the molecular weight of the gases. Hence, the reduction in specific impulse in the oxygen-rich mixtures tends to be less than the reduction in the fuel-rich mixtures. This explanation is strengthened by the fact that ratios greater than unity were obtained only at mixture ratios W_O/W_F greater than stoichiometric.

When ethyl alcohol is used as a coolant (fig. 12(b)), there is again a decrease in impulse ratio with increasing coolant flow in the range of mixture ratios from 1.1 to 1.6; for example, for a coolant flow of 15 percent, specific impulse is reduced approximately 4 percent. For mixture ratios less than 1.1, the data are inconclusive. It was assumed that alcohol and ammonia were equivalent in comparing cooled with uncooled performance; therefore, it is expected that the corrected reduction in specific impulse would be less than that indicated.

The impulse ratio of the cooled engine was greater than unity in the range of mixture ratios from 1.1 to 1.6 for ammonia coolant flows up to approximately 11 percent (fig. 12(c)); beyond this flow there was a slight decrease in performance with increased coolant flow, for example, at a coolant flow of 15 percent, specific impulse was reduced approximately 2 percent. In the range of mixture ratios greater than 1.6, the impulse ratio of the cooled engine was greater than unity up to approximately 13-percent coolant flow.

For ammonia-coolant flows less than about 10 percent, ratios greater than unity are obtained rather consistently in both mixture-ratio ranges. These phenomena suggest the possibility that injection of part of the fuel along the wall may lead to higher combustion efficiencies than are obtained when all of the fuel is injected in the

conventional manner. The cause probably lies in a broadening of the combustion zone and hence more complete combustion prior to expansion through the nozzle.

CONCLUDING REMARKS

The results of this investigation indicate that rocket-engine chambers can be film cooled, in the absence of simultaneous external cooling, with relatively small proportions of fuel and with little or no loss in specific impulse. Thus, lower pressure drops and engine weights may be attained by the elimination of regenerative cooling jackets. It appears that introduction of the coolant at several stations in the chamber would be preferable to introduction of the coolant at a single station. Finally, the lower wall temperatures attained with film cooling make the use of nonstrategic materials of construction such as carbon steel or aluminum possible.

SUMMARY OF RESULTS

Internal film cooling of the chamber of a 64-inch characteristic length, 1000-pound thrust, liquid-ammonia - liquid-oxygen rocket engine was investigated at chamber pressures from about 220 to 270 pounds per square inch absolute and oxidant-fuel mixture ratios from 0.8 to 2.0. Three coolants were studied: water, 2 to 7.5 percent of total flow; ethyl alcohol, 5 to 15 percent; and anhydrous liquid ammonia, 3 to 21 percent.

The results of this investigation can be summarized as follows:

1. Data for estimating film-coolant requirements of cylindrical rocket chambers, for the case where the propellant injector is similar to that used in this investigation, were obtained.

2. Over a comparable range of coolant flows, film-cooled lengths were obtained which were as much as twice those predicted from data previously obtained in a steady-flow film cooling duct.

3. With water as a coolant, a flow equal to approximately 5 percent of total flow was required to completely cool the 4-inch inside-diameter, 8.5-inch-long test section of the chamber; with ethyl alcohol, approximately 15 percent was required; and with anhydrous liquid ammonia, approximately 9 percent was required.

4. Performance data of the ammonia-oxygen system were obtained in an uncooled engine of approximately the same dimensions as the cooled engine, and, when corrected to 250 pounds per square inch absolute chamber pressure, indicated a maximum specific impulse of 220 pound seconds per pound at an oxidant-fuel mixture ratio of 1.4.

5. Over a range of mixture ratios from 1.1 to 1.6, the effect of film cooling on performance is as follows for the coolants and flows indicated: water, 5 percent of total flow, 4 percent reduction in specific impulse; ethyl alcohol, 15 percent of total flow, 4 percent reduction in specific impulse; anhydrous liquid ammonia, no reduction in specific impulse up to coolant flows of 11 percent, and only a 2 percent reduction in specific impulse at a flow of 15 percent.

Lewis Flight Propulsion Laboratory,
National Advisory Committee for Aeronautics,
Cleveland, Ohio.

REFERENCES

1. Bowling, A. G.: Use of Sweat Cooling to Prevent Build-up of Oxide in a Combustion Chamber. Tech. Note No. AERO. 1978, S. D. 86, British R.A.E., Nov. 1948.
2. Duwez, Pol, and Wheeler, H. L., Jr.: An Experimental Study of Sweat Cooling with Nitrogen and Hydrogen. Prog. Rep. No. 4-47, Power Plant Lab. Proj. No. MX801, Jet Prop. Lab., C.I.T., Sept. 24, 1947. (AMC Contract No. W-535-ac-20260, Ordnance Dept. Contract No. W-04-200-ORD-455).
3. Duwez, Pol, and Wheeler, H. L., Jr.: Heat-Transfer Measurements in a Nitrogen Sweat-Cooled Porous Tube. Prog. Rep. No. 4-48, Power Plant Lab. Proj. No. MX801, Jet Prop. Lab., C.I.T., Nov. 6, 1947. (AMC Contract No. W-535-ac-20260, Ordnance Dept. Contract No. W-04-200-ORD-455).

4. Rannie, W. D.: A Simplified Theory of Porous Wall Cooling. Prog. Rep. No. 4-50, Power Plant Lab. Proj. No. MX801, Jet Prop. Lab., C.I.T., Nov. 24, 1947. (AMC Contract No. W-535-ac-20260, Ordnance Dept. Contract No. W-04-200-ORD-455).
 5. Canright, Richard B.: Preliminary Experiments of Gaseous Transpiration Cooling of Rocket Motors. Prog. Rep. No. 1-75, Power Plant Lab. Proj. No. MX801, Jet Prop. Lab., C.I.T., Nov. 24, 1948. (AMC Contract No. W-535-ac-20260, Ordnance Dept. Contract No. W-04-200-ORD-455).
 6. Wheeler, H. L., Jr.: The Influence of Wall Material on the Sweat-Cooling Process. Prog. Rep. No. 4-90, Jet Prop. Lab., C.I.T., May 3, 1949 (Ordnance Dept. Contract No. W-04-200-ORD-455).
 7. Duwez, Pol, and Wheeler, H. L.: Preliminary Experiments on the Sweat-Cooling Method. Prog. Rep. No. 3-13, Power Plant Lab. Proj. No. MX527, Jet Prop. Lab., C.I.T., July 18, 1946. (ATSC Contract No. W-33-038-ac-4320).
 8. Sloop, J. L., and Kinney, George R.: Internal-Film Cooling of Rocket Nozzles. NACA RM E5A29a, 1948.
 9. Schurman, Glenn A.: An Investigation of Film Cooling in a Flame Tube. Prog. Rep. No. 1-74, Power Plant Lab. Proj. No. MX801, Jet Prop. Lab., C.I.T., June 30, 1948 (AMC Contract No. W-535-ac-20260, Ordnance Dept. Contract No. W-04-200-ORD-455).
 10. Boden, Robert H.: Film Cooling. Prog. Rep. No. 4-19, Air Lab. Proj. No. MX121, Jet Prop. Lab., C.I.T., Jan. 6, 1946. ATSC Contract No. W-535-ac-20260, ASF Ordnance Dept. Contract No. W-04-200-ORD-455).
 11. Kinney, George R., and Sloop, John L.: Internal Film Cooling Experiments in a 4-inch Duct with Gas Temperatures to 2000° F. NACA RM E50F19, 1950.
 12. McAdams, William H.: Heat Transmission. McGraw-Hill Book Co., Inc., (New York), 2d ed., 1942, pp. 63, 241.
 13. West, F. L.: An Approximate Method for Predicting the Heat Transfer in a Cooled Rocket Nozzle. Tech. Aero. Note 1891, British R.A.E., May 1947.
 14. Huff, Vearl N., and Morrell, Virginia E.: General Method for Computation of Equilibrium Composition and Temperature of Chemical Reactions. NACA TN 2113, 1950.
- ~~CONFIDENTIAL~~

- 2178
15. Canright, R. B.: The Use of the Ammonia-Liquid Oxygen Reaction in Rocket Motors, Including a Discussion of Noncarbonaceous Propellants. Prog. Rep. No. 1-49, Air. Lab. Proj. No. MX121, Jet Prop. Lab., C.I.T., Oct. 31, 1946. (AMC Contract No. W-535-ac-20260).
 16. Perry, John H.: Chemical Engineers' Handbook. McGraw-Hill Book Co., Inc., (New York), 2d ed., 1941.
 17. Chapman, Sydney, and Cowling, T. G.: The Mathematical Theory of Non-Uniform Gases. Cambridge Univ. Press (Cambridge, England), 1939.
 18. Gilbert, Mitchell: Estimation of the Viscosity, Conductivity, and Diffusion Coefficients of O, H, N, and OH. Memo. No. 4-51, Power Plant Lab. Proj. No. MX527, Jet Prop. Lab., C.I.T., July 6, 1949. (AMC Contract No. W-33-038-ac-4320, Ordnance Dept. Contract No. W-04-200-ORD-455).
 19. Huff, Vearl N., and Gordon, Sanford: Tables of Thermodynamic Functions for Analysis of Aircraft-Propulsion Systems. NACA TN 2161, 1950.
 20. Sutton, George P.: Rocket Propulsion Elements. John Wiley & Sons, Inc., (New York), 1949, p. 85.
 21. McAdams, William H.: Heat Transmission. Radiant Heat Transmission, chap. III, by Hoyt C. Hottel, McGraw-Hill Book Co., Inc., (New York), 2d ed., 1942, pp. 45-86.
 22. Anon.: Summary Report on Theoretical, Laboratory and Experimental Investigations of High Energy Propellants. Ammonia, vol. I, Rep. No. RMI-293-S1, RMI Proj. No. 293, Reaction Motors, Inc., July 5, 1950. (Navy Contract No. NOa(s) 9469).
- ~~CONFIDENTIAL~~

TABLE I - HEAT-TRANSFER AND ASSOCIATED PERFORMANCE DATA FOR ROCKET-ENGINE COMBUSTION CHAMBER FILM COOLED WITH WATER

Run	Oxidant flow W_o (lb/sec)	Fuel flow W_f (lb/sec)	Coolant flow W_l (lb/sec)	Thrust F (lb)	Chamber pressure P_c (lb/sq in. abs.)	Oxidant-fuel ratio $\frac{W_o}{W_f}$	Coolant $100 W_l$ $\frac{W_o+W_f+W_l}{W_o}$ (percent)	Theoretical specific impulse I (lb-sec/lb)	Impulse efficiency η_I	Average liquid-cooled length to diameter ratio L/D	Total heat transfer per pound of coolant q_t (Btu/lb)	Radiation heat transfer per pound of coolant q_r (Btu/lb)	Convective heat transfer per pound of coolant q_c (Btu/lb)
Vertical-slot coolant injector													
1	2.49	1.55	0.189	885	255	1.61	4.47	244	0.86	2.09	876	97	779
2	2.55	1.63	.181	935	262	1.56	4.15	247	.87	1.91	868	106	760
3	2.50	1.52	.15	896	250	1.64	3.60	242	.89	1.40	876	86	790
4	2.44	1.72	.154	892	256	1.42	3.57	250	.82	1.44	866	72	794
5	2.22	1.48	.147	880	250	1.50	3.82	247	.93	1.59	866	150	716
6	2.55	1.54	.091	892	252	1.66	2.18	242	.90	.69	896	71	825
7	2.48	1.44	.090	896	257	1.72	2.24	240	.93	.97	926	136	790
Tangential-slot coolant injector													
8	2.18	1.55	0.184	892	252	1.41	4.70	250	0.91	1.85	876	144	732
9	2.30	1.52	.184	874	248	1.51	4.60	246	.91	2.04	871	135	736
10	2.55	1.46	.204	915	260	1.75	4.84	239	.91	2.01	856	125	731
11	2.50	1.50	.208	915	260	1.67	4.94	242	.895	2.14	856	135	721



TABLE II - HEAT-TRANSFER AND ASSOCIATED PERFORMANCE DATA FOR ROCKET-ENGINE COMBUSTION CHAMBER FILM COOLED WITH FUEL;
VERTICAL-SLOT COOLANT INJECTOR

Run	Oxidant flow \dot{W}_o (lb/sec)	Fuel flow \dot{W}_f (lb/sec)	Coolant flow \dot{W}_c (lb/sec)	Thrust F (lb)	Chamber pressure P_c (lb/sq in. abs.)	Oxidant-fuel ratio $\frac{\dot{W}_o}{\dot{W}_f + \dot{W}_c}$	Coolant 100 W, $\dot{W}_o + \dot{W}_f + \dot{W}_c$ (percent)	Theoretical specific impulse I (lb-sec/lb)	Impulse efficiency η_I	Average liquid-cooled length to diameter ratio L/D	Total heat transfer per pound of coolant q_t (Btu/lb)	Radiation heat transfer per pound of coolant q_r (Btu/lb)	Convective heat transfer per pound of coolant q_c (Btu/lb)
Coolant, ethyl alcohol ^a													
12	2.47	1.52	0.569	965	262	1.18	12.5	247.5	0.86	1.40	309	16	293
13	2.40	1.57	.610	941	256	1.10	13.3	243	.85	1.59	304	14	280
14	2.48	1.53	.587	978	262	1.17	12.8	247.5	.86	1.71	309	19	290
15	2.51	1.46	.605	945	255	1.12	13.8	244	.885	1.81	320	19	301
16	1.81	1.85	.605	812	225	.80	14.9	219	.91	2.10	346	11	335
17	2.42	1.32	.615	985	265	1.25	14.1	251	.90	1.74	316	25	291
18	2.53	1.55	.610	958	260	1.17	15.0	247.5	.825	1.77	304	18	288
19	2.39	1.61	.503	947	258	1.13	11.2	246	.85	1.59	290	20	270
20	2.50	1.50	.501	977	265	1.25	13.0	232.5	.88	2.04	330	16	314
21	2.08	1.62	.551	860	235	1.41	8.7	252	.84	1.44	304	30	274
22	2.70	1.51	.421	968	263	1.37	9.5	251	.87	1.58	304	32	272
23	2.58	1.45	.420	979	266	1.41	8.7	227	.89	1.97	348	13	335
24	1.80	1.71	.466	781	218	.85	11.7	227	.89	1.97	348	13	335
25	2.67	1.43	.375	980	266	1.48	8.4	249	.88	1.08	289	26	263
26	2.61	1.63	.370	989	268	1.31	8.0	249.5	.86	1.02	299	22	277
27	1.80	1.74	.371	775	217	.85	9.5	225	.89	1.88	340	18	322
28	2.72	1.53	.240	972	265	1.54	5.35	248	.875	1.01	299	58	261
29	2.58	1.43	.260	960	262	1.53	6.1	248	.91	.94	295	58	257
30	2.67	1.46	.223	981	268	1.59	5.1	247	.91	1.00	304	52	252
Coolant, anhydrous liquid ammonia													
31	2.38	1.50	0.76	996	270	1.05	16.4	244	0.87	1.97	501	18	485
32	2.22	1.235	.865	823	230	1.08	20.0	239.5	.80	2.01	503	7.5	495.5
33	2.74	1.145	.625	988	269	1.55	13.9	247.5	.885	1.95	502.5	27	475.5
34	2.79	1.125	.570	962	262	1.64	12.7	244	.88	2.03	502.5	30	472.5
35	2.63	1.15	.582	950	258	1.54	12.95	247	.89	1.94	502.5	31	471.5
36	2.58	1.20	.495	925	253	1.55	11.4	246	.88	1.94	502.5	34.5	468
37	2.57	1.16	.465	920	253	1.58	11.1	244	.90	1.86	499	36.5	462.5
38	2.80	1.175	.460	958	257	1.71	10.4	239	.89	1.84	501	33	468
39	2.46	1.11	.413	925	253	1.62	10.4	243	.955	1.82	502.5	55	447.5
40	2.68	1.07	.413	904	248	1.81	9.9	235	.92	1.86	502.5	45	457.5
41	2.58	1.185	.413	914	252	1.61	9.9	243.5	.90	1.86	501	43	458
42	2.66	1.20	.335	931	255	1.73	8.0	239.5	.93	1.40	502.5	47	455.5
43	2.44	1.175	.342	919	255	1.61	8.7	244	.95	1.75	501	63	438
44	2.42	1.305	.352	938	257	1.45	8.6	250	.92	1.76	502.5	55	447.5
45	3.20	1.20	.317	934	257	2.11	6.7	217.5	.91	1.44	499	26	473
46	2.72	1.44	.545	811	228	1.52	7.7	243	.74	1.51	499	14	485
47	2.48	1.30	.255	918	253	1.59	6.3	244.5	.93	.59	502.5	26	476.5
48	1.96	1.54	.295	788	222	1.08	7.7	240	.86	1.69	503	34	489
49	2.44	1.29	.293	910	250	1.54	7.3	245.5	.92	1.48	502.5	54	448.5
50	2.42	1.32	.293	922	252	1.50	7.3	246	.93	1.64	499	62	437
51	2.39	1.44	.310	855	239	1.37	7.5	248.5	.83	1.49	499	31	468
52	2.38	1.32	.282	918	252	1.49	7.1	247.5	.935	1.31	503	53	450
53	2.39	1.295	.282	928	255	1.52	7.1	248	.94	1.33	501	59	442
54	2.54	1.30	.281	936	257	1.61	6.8	244.5	.93	1.39	498	56	440
55	2.52	1.39	.22	919	252	1.57	5.3	245	.91	1.05	499	47	452
56	2.02	1.53	.285	786	221	1.11	7.4	240.5	.85	1.56	488	27	461
57	2.38	1.47	.165	895	247	1.46	4.1	248	.90	.84	499	50	449
58	2.58	1.29	.172	907	252	1.77	4.3	237	.95	.87	475	58	417
59	2.58	1.34	.130	905	252	1.76	3.2	237	.94	.64	475	55.5	419.5

^aTheoretical impulse for alcohol is assumed to be the same as for ammonia.

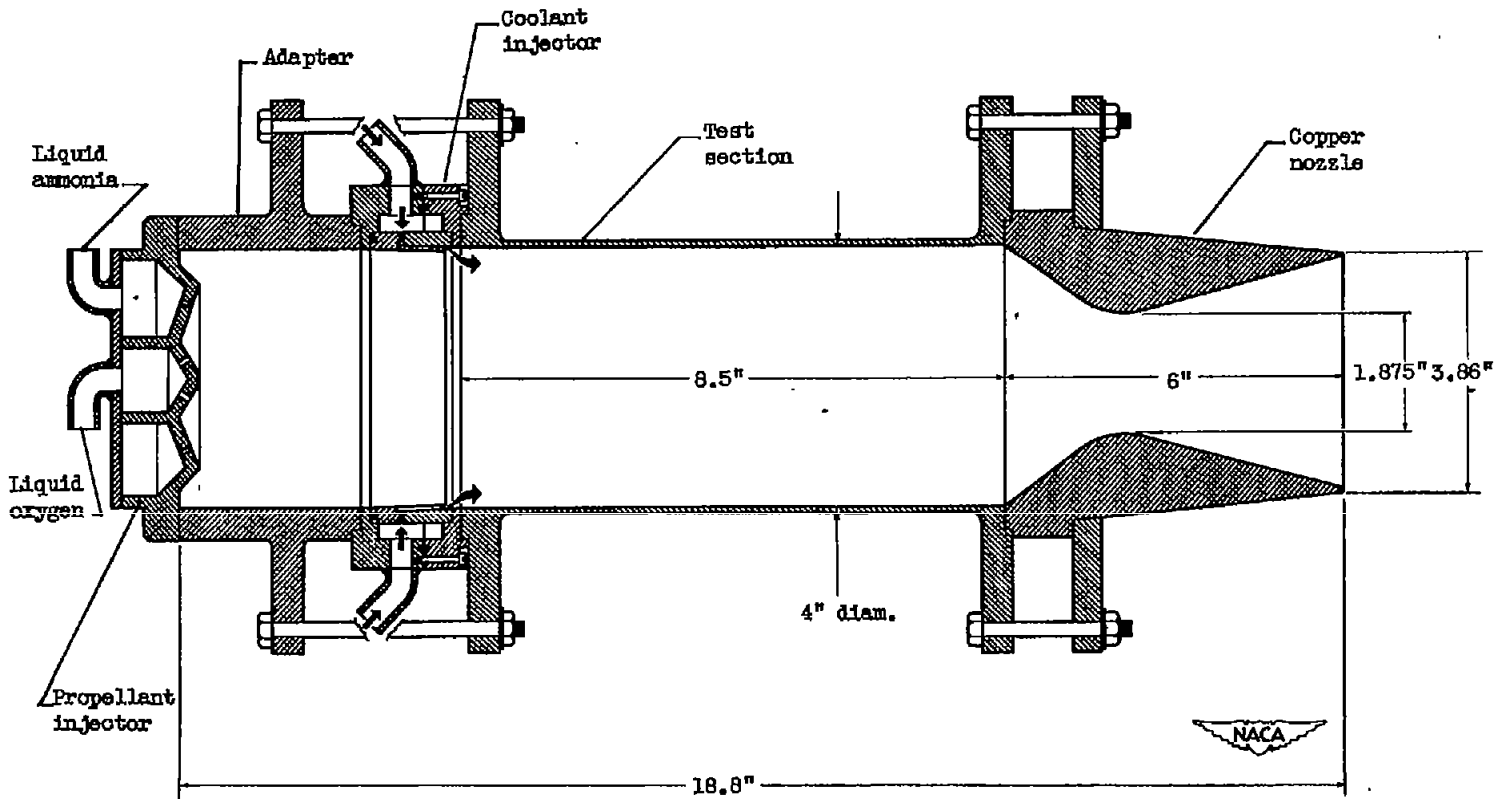


Figure 1. - Diagrammatic sketch of rocket engine used for film-cooling.

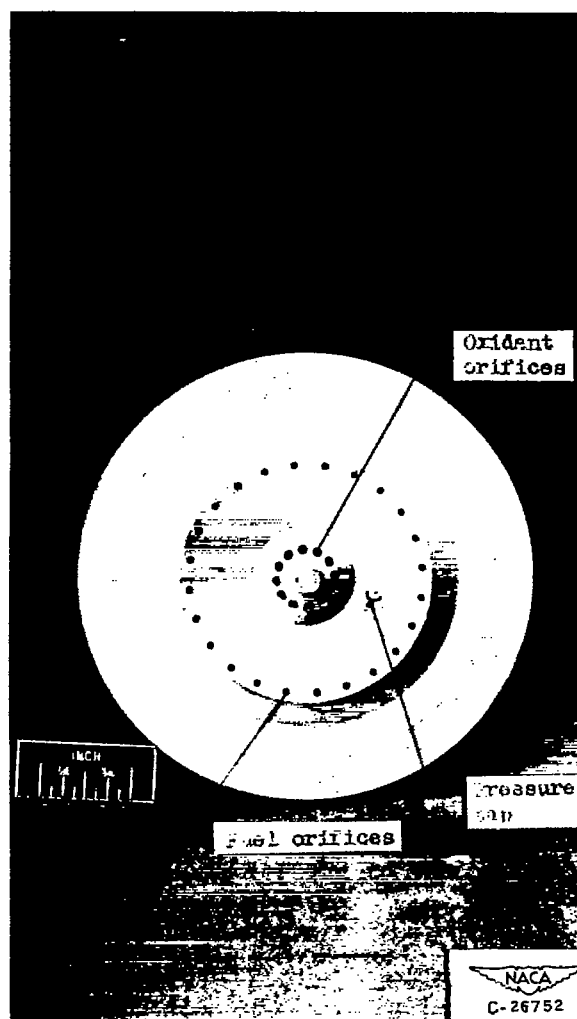


Figure 2. - Propellant injector.

1

2

3

4

5

6

7

8

9

10

11

12

13

14

15

16

17

18

19

20

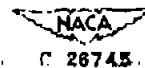


Figure 3. - Component parts of slot-type coolant injector.

6

7

8

9

10

11



Figure 4. - Thin-walled stainless-steel test section.

1870

1

2

3

4

5

6

7

1871

1872

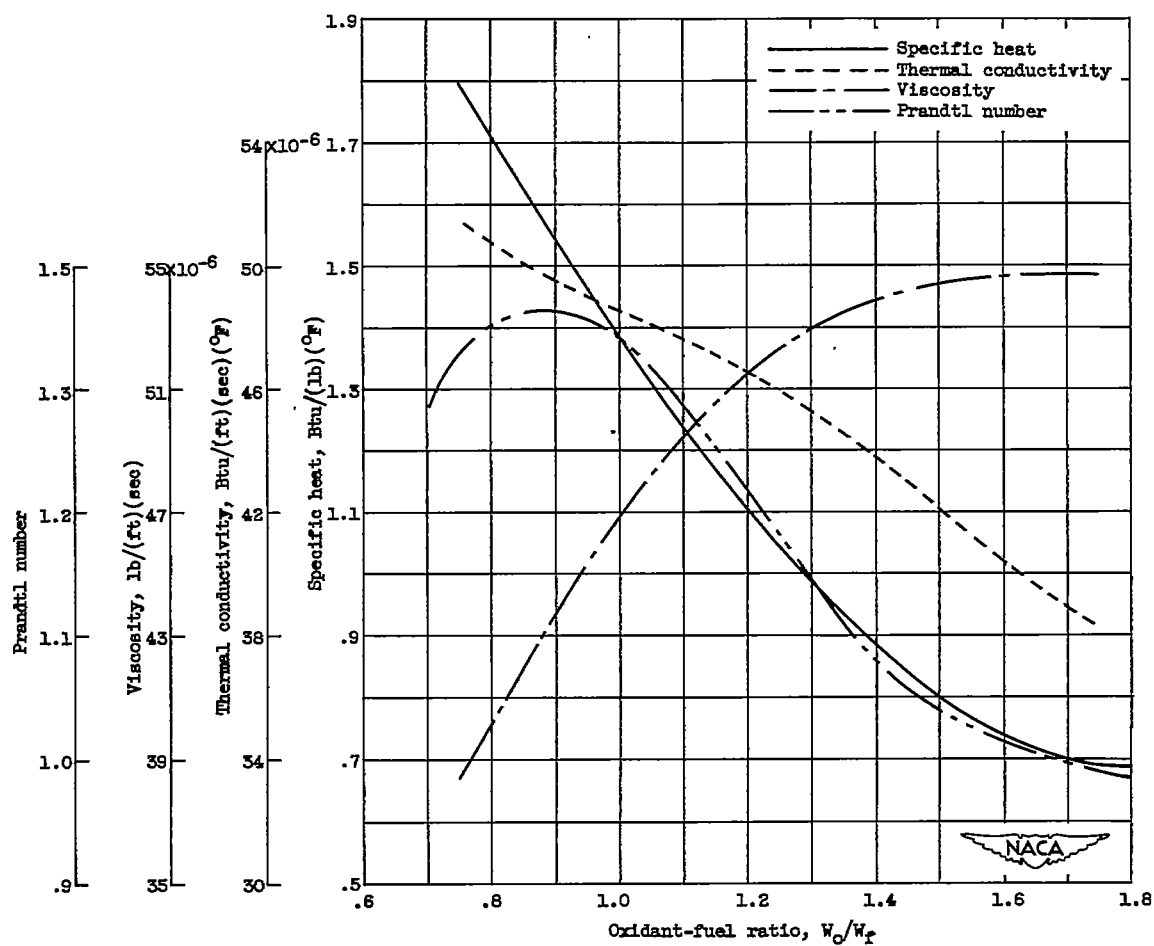


Figure 5. - Properties of combustion gases of ammonia-oxygen system based on theoretical compositions.

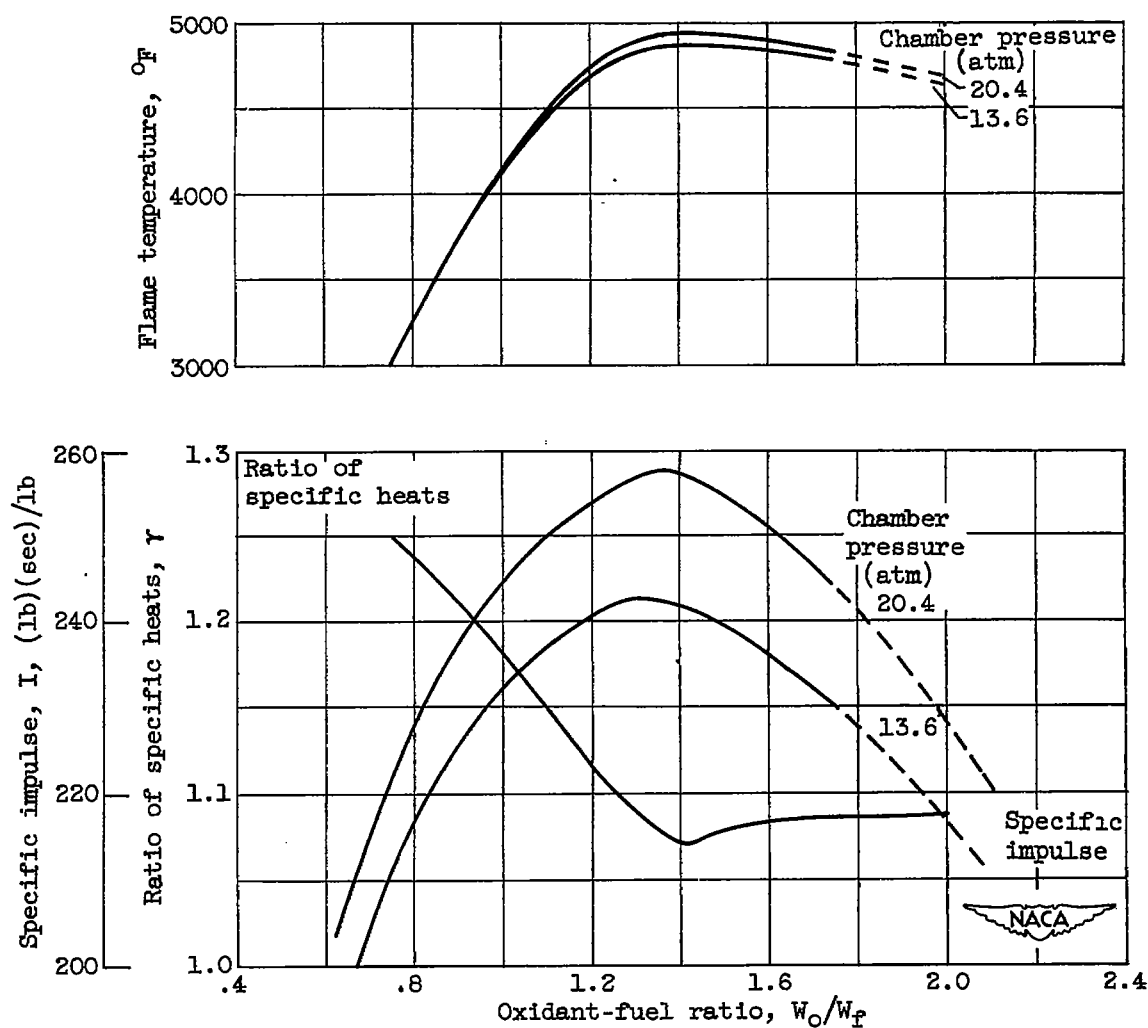
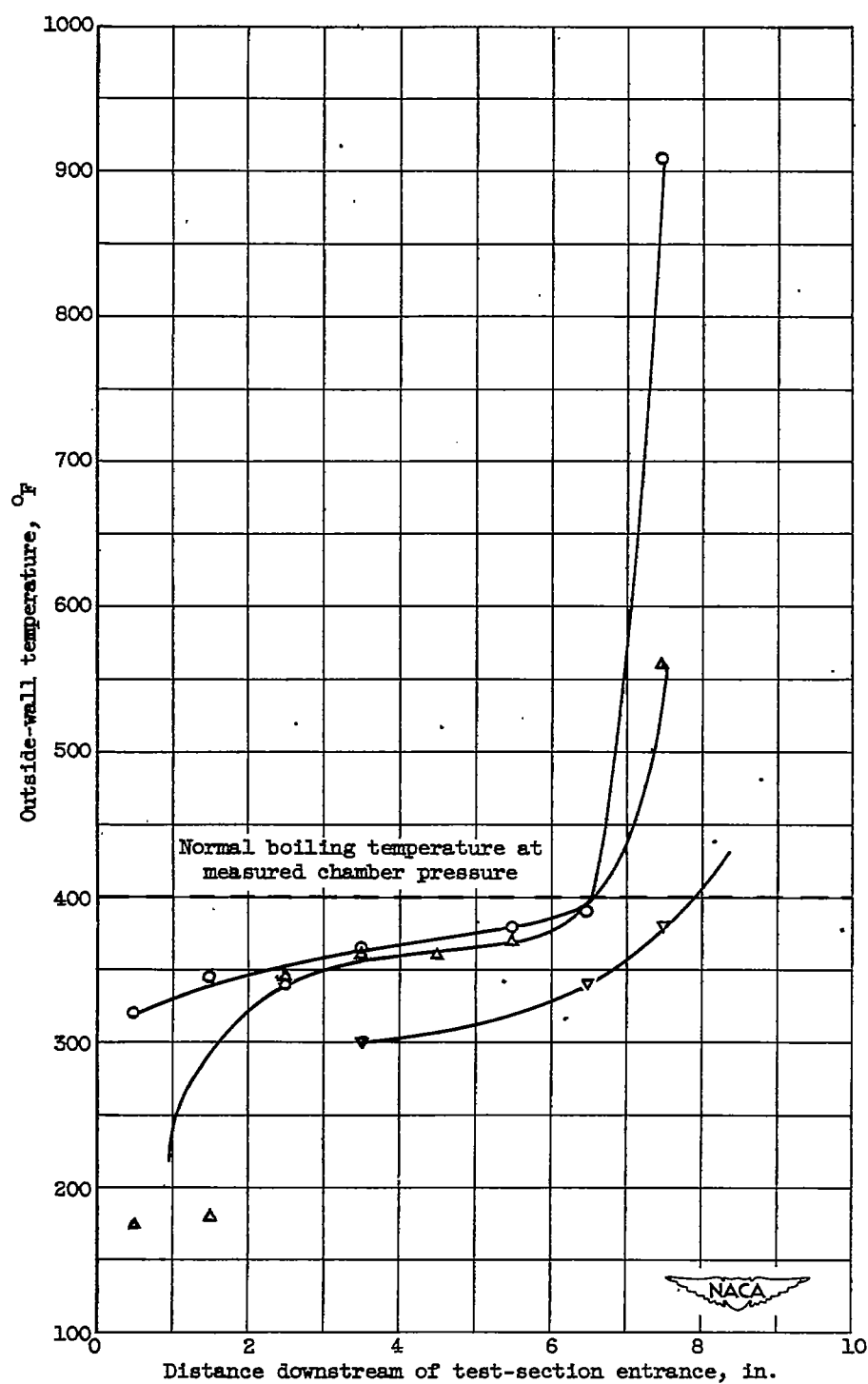
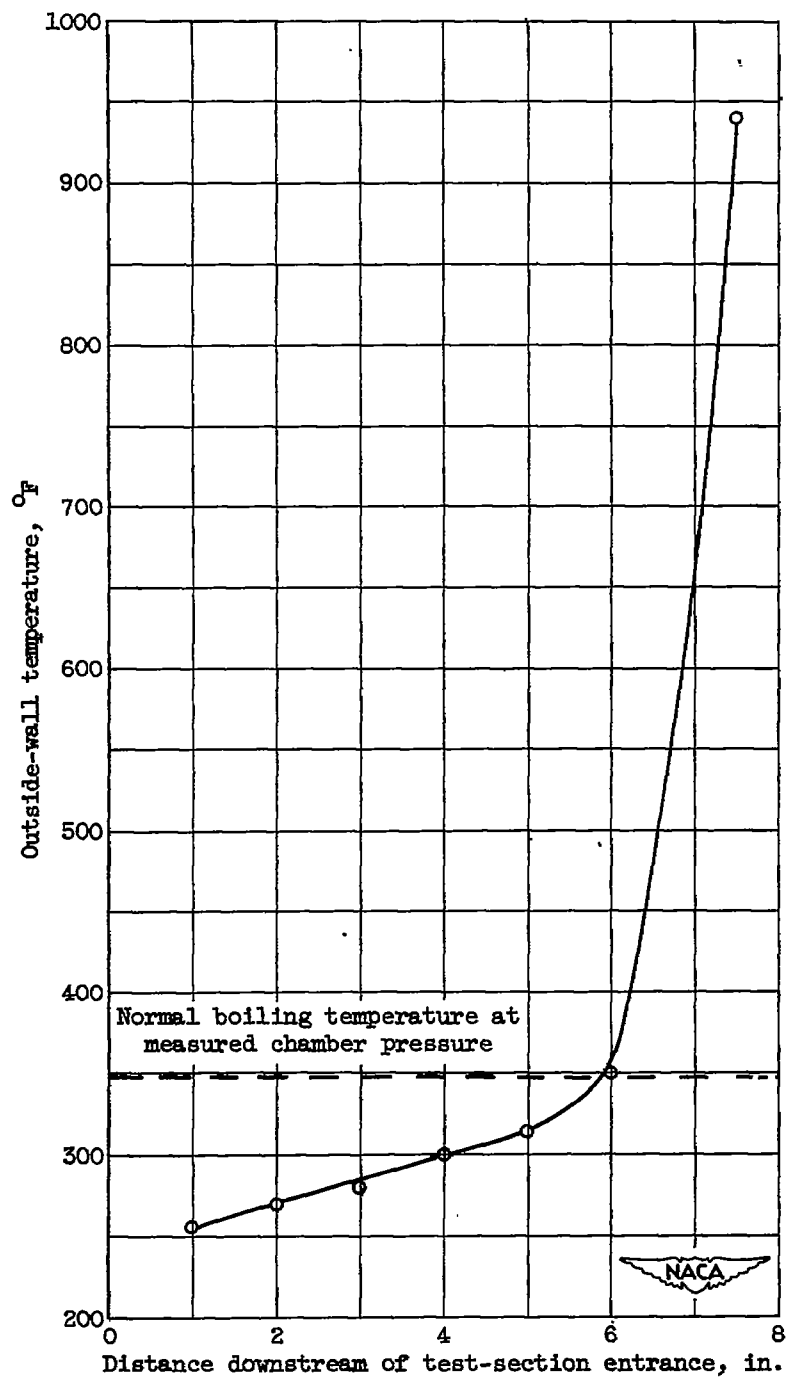


Figure 6. - Theoretical values of specific impulse (expansion to 1 atm), flame temperature, and ratio of specific heats (20.4 atm).



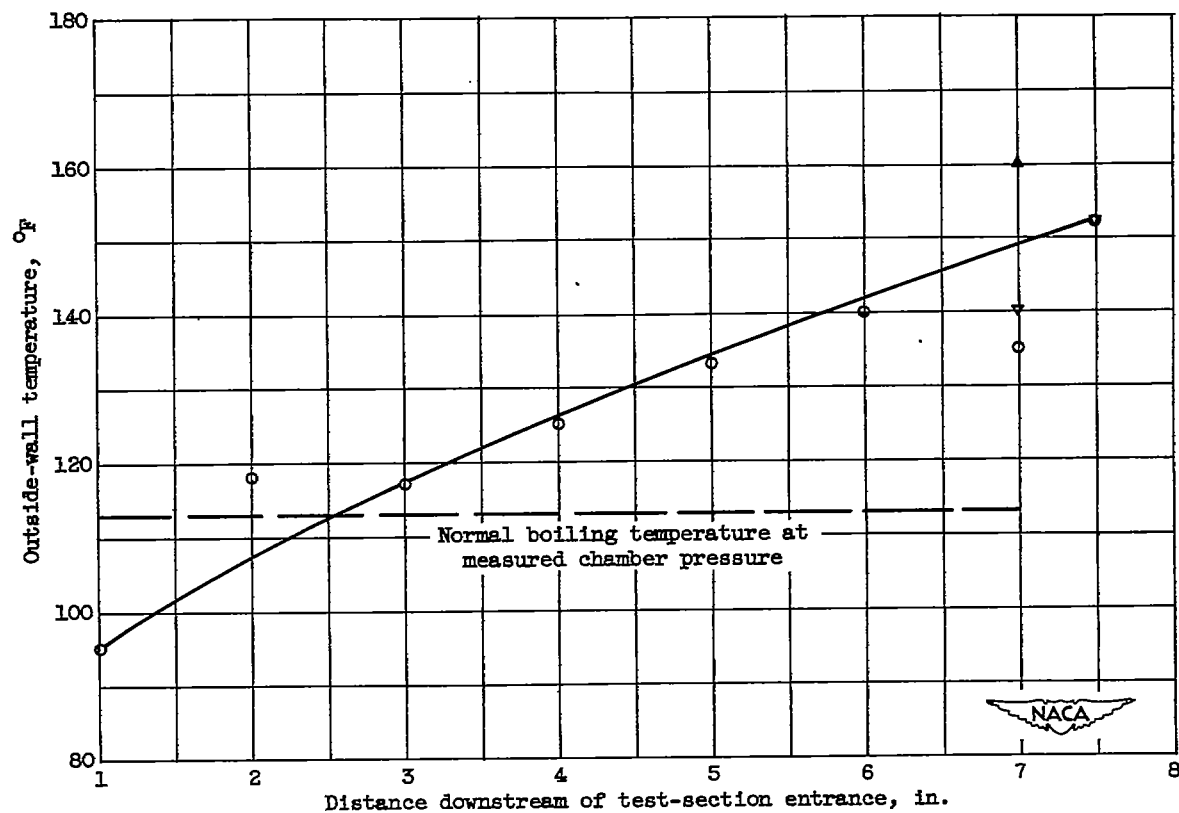
(a) Coolant, water.

Figure 7. - Typical wall-temperature survey of film-cooled test section. Symbols refer to different longitudinal rows of thermocouples.



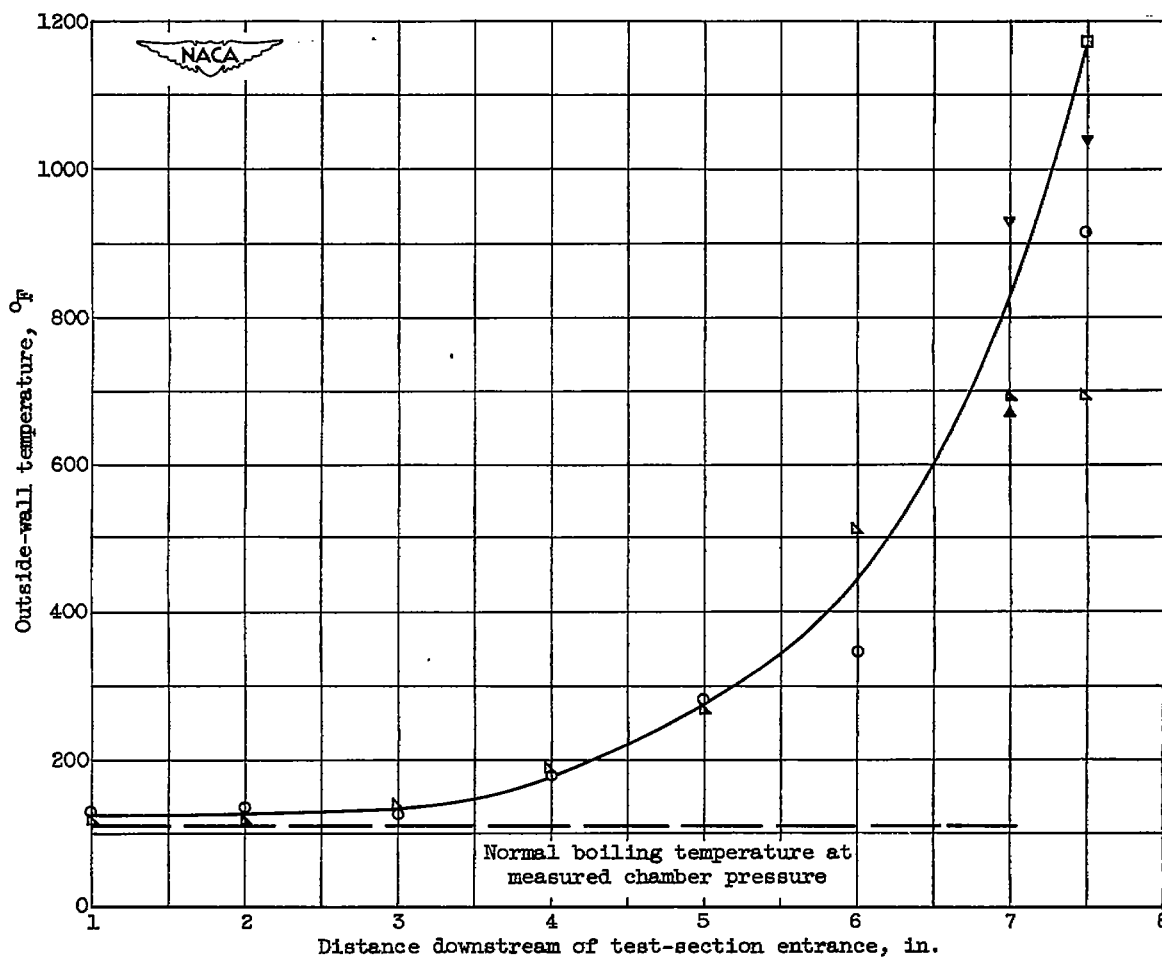
(b) Coolant, alcohol.

Figure 7. - Concluded. Typical wall-temperature survey of film-cooled test section. Symbols refer to different longitudinal rows of thermocouples.



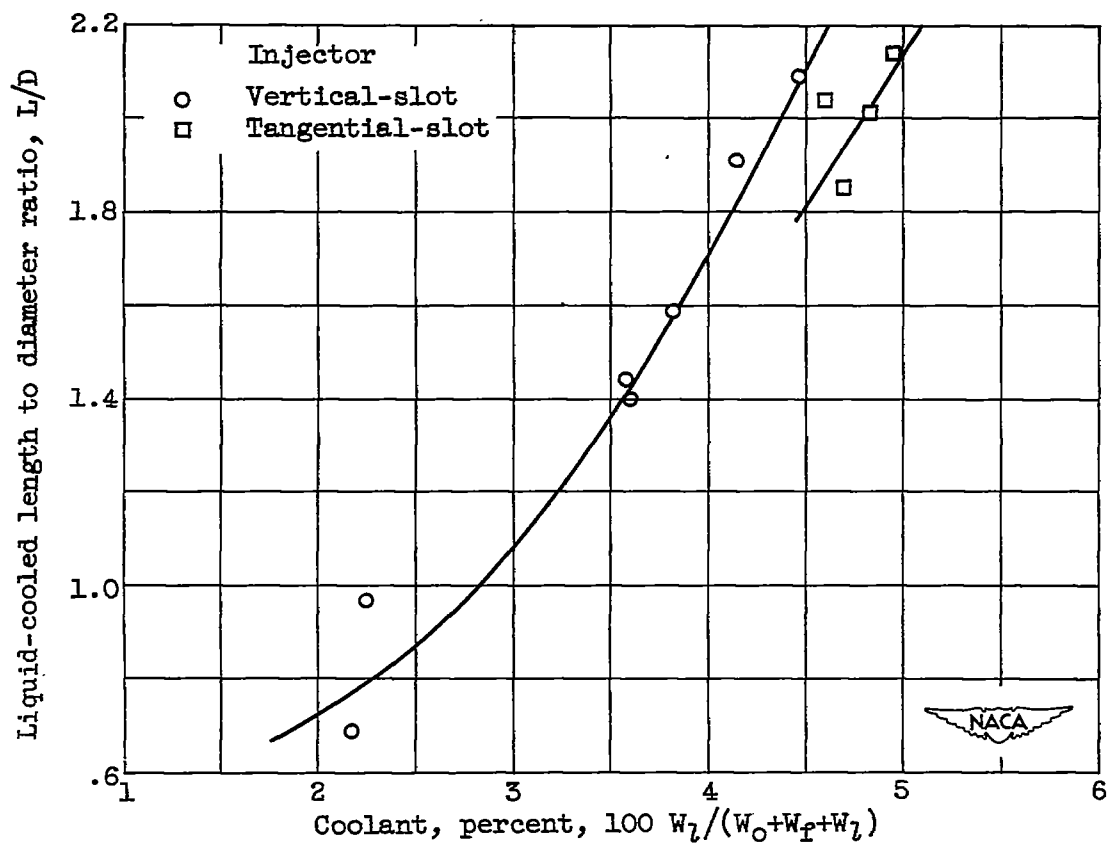
(a) Completely cooled section.

Figure 8. - Typical wall-temperature survey of test section film cooled with ammonia. Symbols refer to different longitudinal rows of thermocouples.



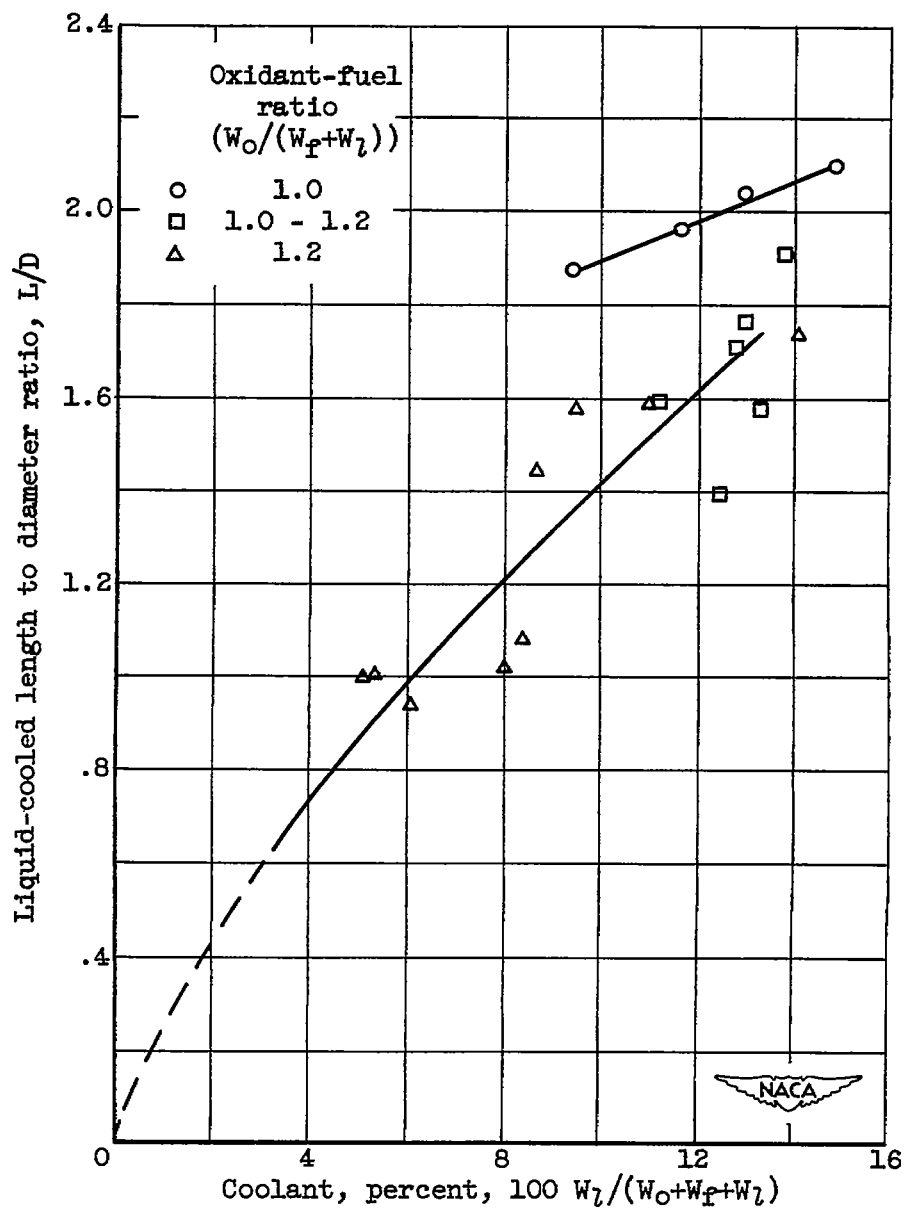
(b) Partially cooled section.

Figure 8. - Concluded. Typical wall-temperature survey of test section film cooled with ammonia. Symbols refer to different longitudinal rows of thermocouples.



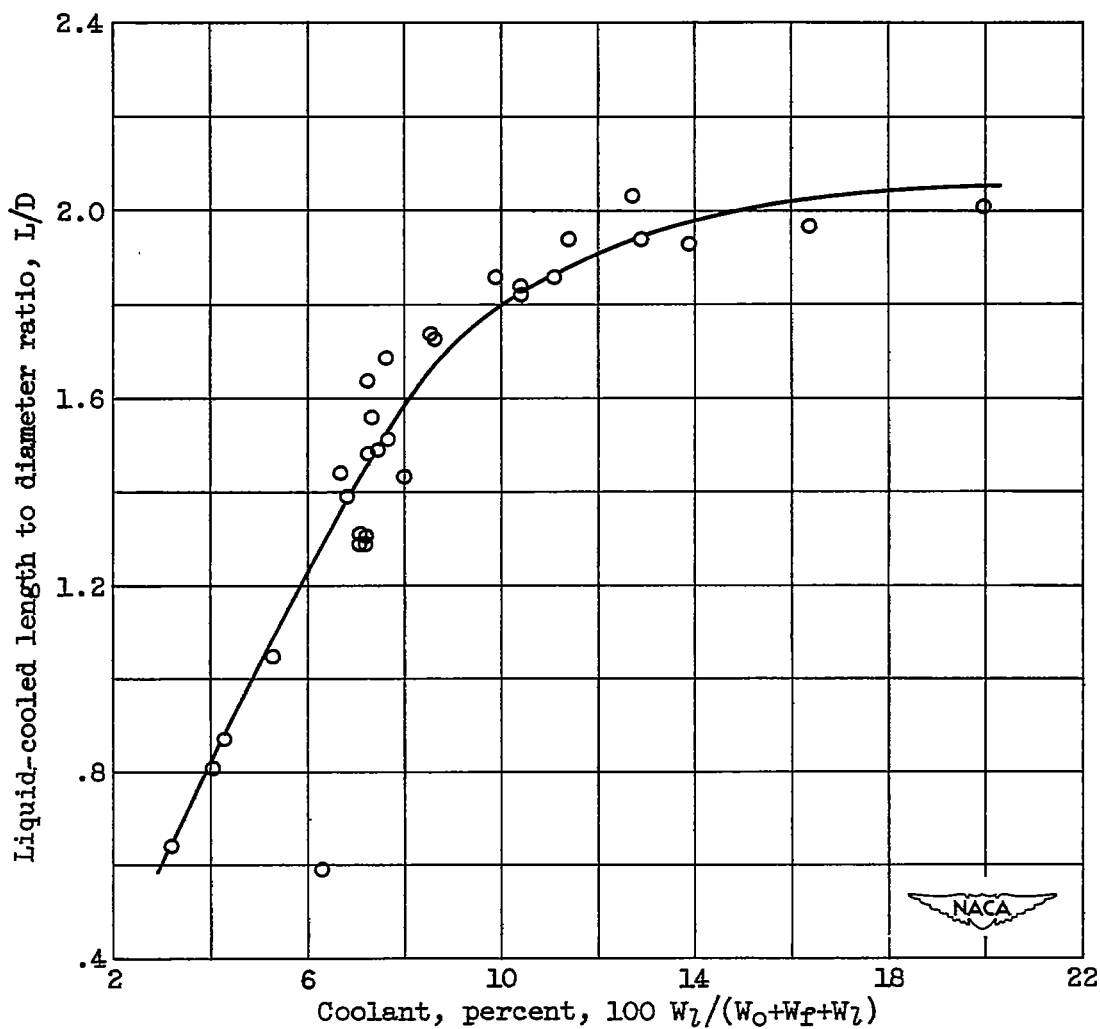
(a) Coolant, water.

Figure 9. - Variation of liquid-cooled length to diameter ratio with percentage of coolant.



(b) Coolant, alcohol; vertical-slot injector.

Figure 9. - Continued. Variation of liquid-cooled length to diameter ratio with percentage of coolant.



(c) Coolant, ammonia; vertical-slot injector.

Figure 9. - Concluded. Variation of liquid-cooled length to diameter ratio with percentage of coolant.

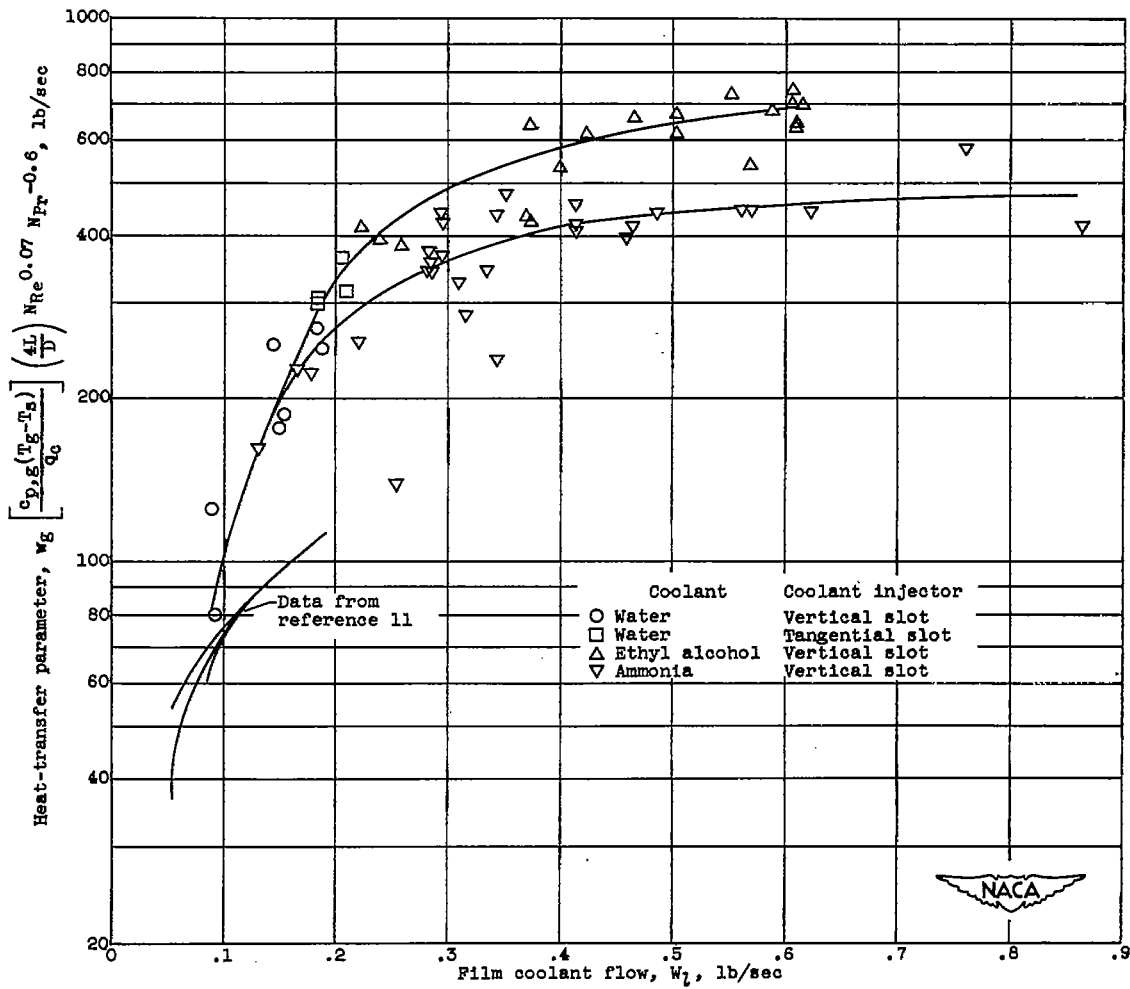


Figure 10. - Gas to film coolant heat-transfer data for ammonia-oxygen propellant system.

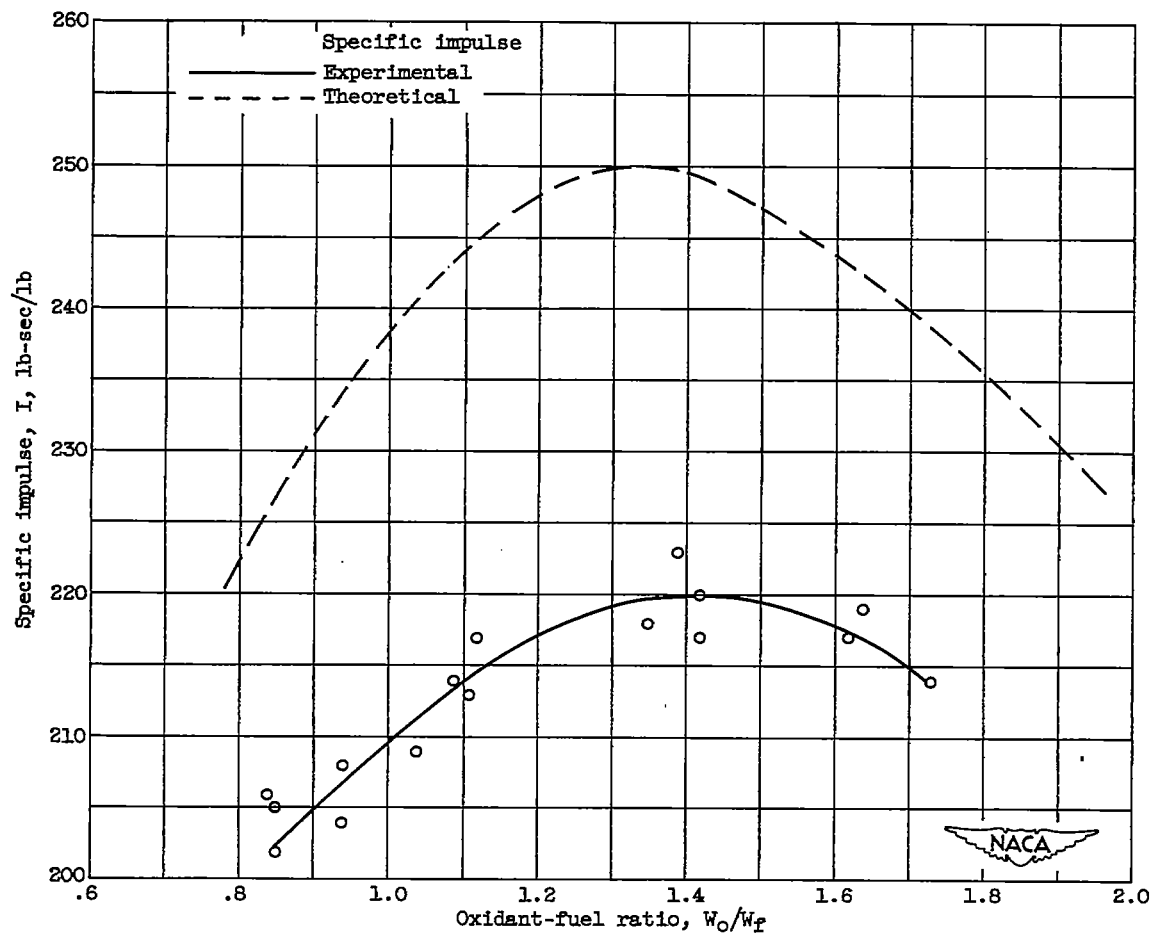
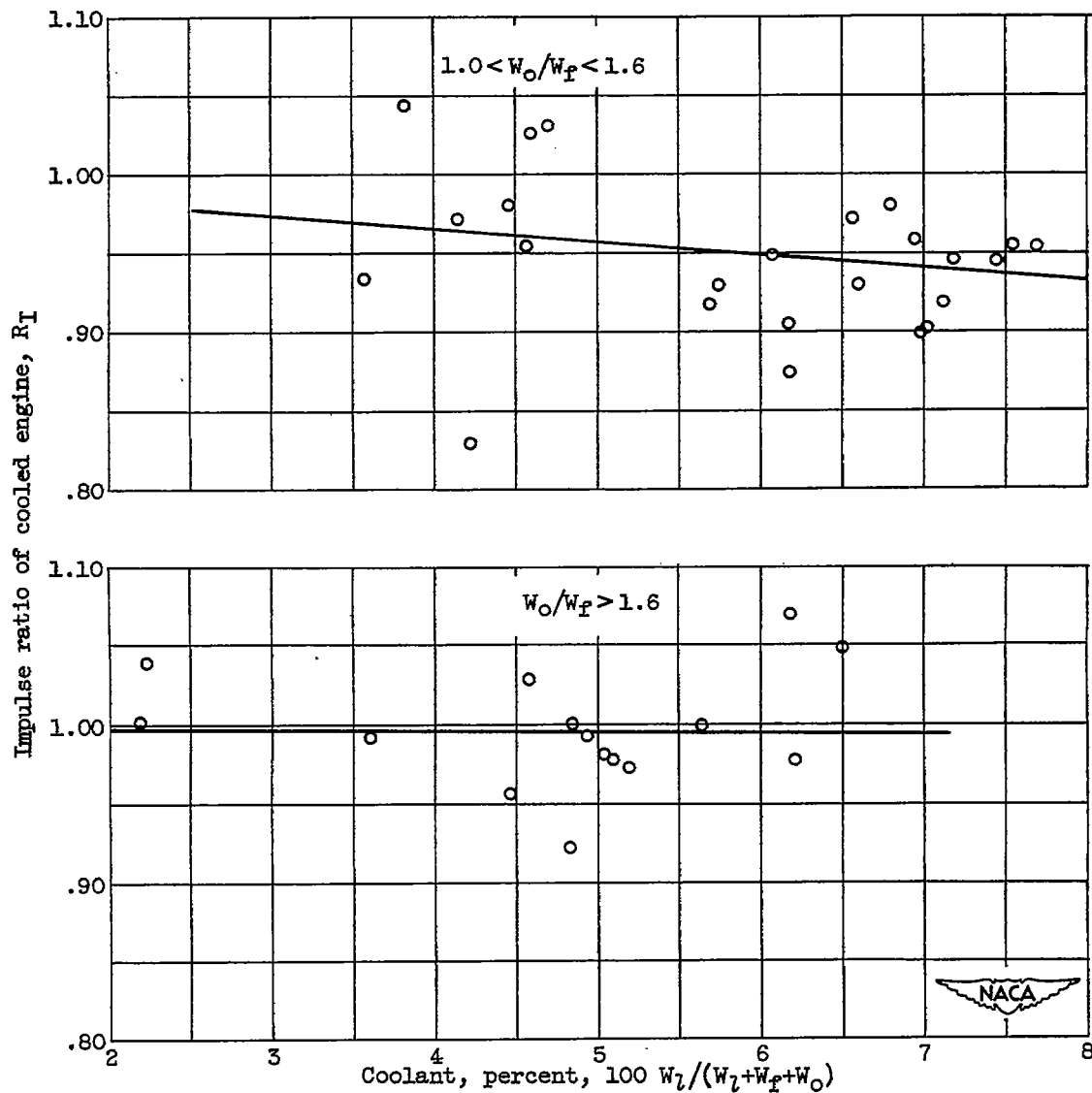
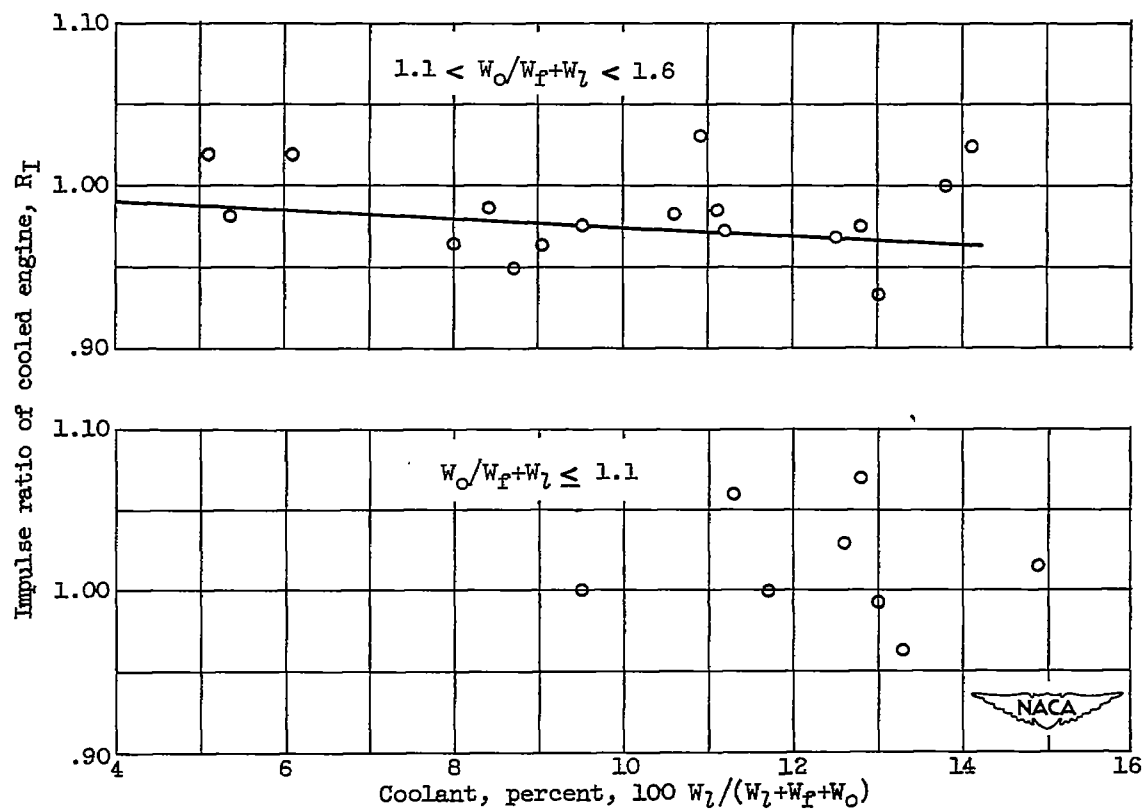


Figure 11. - Experimental specific impulse of ammonia-oxygen system corrected to chamber pressure of 250 pounds per square inch absolute and expanding to 1 atmosphere. Standard propellant injector, characteristic length of engine, 67 inches.



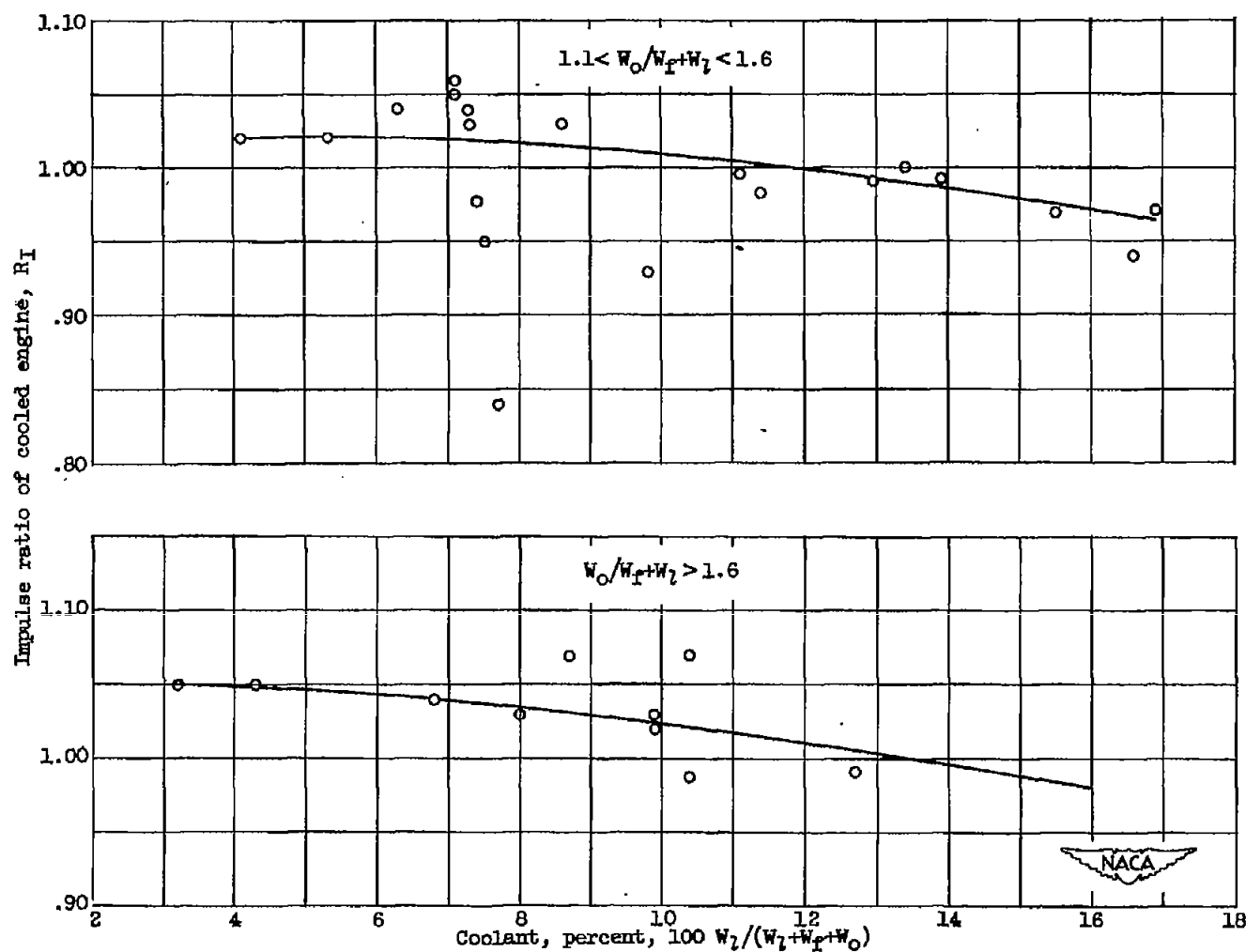
(a) Coolant, water.

Figure 12. - Effect of film cooling on performance of 1000-pound-thrust ammonia-oxygen rocket engine. Chamber pressure, 250 pounds per square inch absolute.



(b) Coolant, ethyl alcohol.

Figure 12. - Continued. Effect of film cooling on performance of 1000-pound-thrust ammonia-oxygen rocket engine. Chamber pressure, 250 pounds per square inch absolute.



(c) Coolant, ammonia.

Figure 12. - Concluded. Effect of film cooling on performance of 1000-pound-thrust ammonia-oxygen rocket engine. Chamber pressure, 250 pounds per square inch absolute.